Regular Article

PHYSICAL CHEMISTRY RESEARCH
Published by the
Iranian Chemical Society
www.physchemres.org
info@physchemres.org

Phys. Chem. Res., Vol. 8, No. 1, 31-44, March 2020
DOI: 10.22036/pcr.2019.198012.1661

Preparation of Phosphorus Doped Graphitic Carbon Nitride Using a Simple Method and Its Application for Removing Methylene Blue

M. Chegeni* and N. Dehghan

Department of Chemistry, Faculty of Science, Ayatollah Boroujerdi University, Boroujerd, Iran

(Received 13 August 2019, Accepted 24 November 2019)

Nowadays, dye pollution arising from industrial activities has become an environment issue. Surface adsorption of pollutants seems to be a promising solution for this problem. In this research, P-doped graphitic carbon nitride was prepared by the facile strategy with phosphoric acid and melamine. The characterization of P-doped graphitic carbon nitride (P-g-C_3N_4) was performed using FT-IR, XRD, SEM and BET analyses. The preparation method was simple, easy and efficient compared to other methods. The as-synthesized P-doped g-C_3N_4 was applied for the adsorption of methylene blue. The results were analyzed using the isotherms of Langmuir and Freundlich. The best fit was resulted from Langmuir isotherm having an R^2 value of 0.98. The maximum adsorption capacity (q_{max}) from the Langmuir isotherm was 100 mg g^{-1} when pH, adsorbent dosage, initial concentration of methylene blue, and contact time are 8, 0.07 g, 8 ppm and 60 min at 18 °C. The adsorption on the P-doped graphitic nitride matched pseudo-second order model. Based on our findings, P-g-C_3N_4 could be an efficient material to adsorb methylene blue.

Keywords: P-doped graphitic carbon nitride, Methylene blue, Adsorption, Isotherm

INTRODUCTION

Recently, environmental pollution has become a major concern for human in worldwide. The development of industries as well as massive population growth is contributing to this plight. The industrial revolution was accompanied by a sudden increase in pollution. Many companies such as food, leather, pharmaceutical and textile industries can produce organic pollutants such as organic dyes. These pigments are toxic, harmful, resistant to degradation, and can result in cancer [1]. Hence, the removal of organic dyes has become an essential topic.

One of the necessary requirements is designing new materials to overcome this problem. Among new polymers, graphitic carbon nitride (g-C_3N_4) has attracted the attention of researchers due to its properties such as physical and chemical stability, and electronic band structure. The graphitic carbon nitride can be synthesized *via* different precursors containing nitrogen [2-3].

Note that graphitic carbon nitride can be applied as an optic device, sensor, photocatalyst, and as an agent to increase the catalytic activity. The photocatalyst activity of g-C_3N_4 can be applied for degradation of pollutants. The unique structure of g-C_3N_4 has specially attracted the attention of scientists trying to improve the building structure of this polymer [4-8].

This semiconductor is cheap and ecofriendly material [5]. In order to obtain the best yield, the modification of graphitic carbon has been studied extensively. This can be achieved by doping atom, adding metal and formation of novel composites to improve adsorption property. Some of these methods include synthesizing V_2O_5/g-C_3N_4 [9], g-C_3N_4/$BiVO_4$ [10], g-C_3N_4/ZnO [11] and g-C_3N_4/$BiPO_4$ [12] composites as well as doping sulfur [13], phosphorus [14] and sodium [15]. Among these procedures, doping atoms can improve the electronic properties to increase the degradation after adsorption on the surface of adsorbent.

*Corresponding author. E-mail: mahdieh.chegeni@abru.ac.ir

Here, delocalization electrons can be developed and this method needs cheap precursors compared to construct new multi-component material. The photocatalytic and adsorption activities can be increased by addition of small amounts of phosphorus [16-17]. The photoexcited electron-hole pairs can decrease the yield of photocatalyst activity of non-doped carbon nitride graphitic. However, the photocatalytic efficiency of g-C_3N_4 is limited due to its high recombination of photo-excited electron-hole pairs. Based on the analysis and adsorption results, the porosity of g-C_3N_4 can increase the surface area through doping P atom on graphitic carbon nitride.

The P-doped graphitic carbon nitride was obtained by melamine and melamine phosphate ester polymer [14]. In another strategy, an ionic liquid, $BmimPF_6$, was employed as a dopant to improve the adsorption activity of graphitic carbon nitride compared to non-doped polymer. In general, the utilized methods have some disadvantages such as expensive and unconventional precursors, as well as difficult recovery and purification [18].

This study contains the following subjects: (i) Preparation of phosphorus-doped graphitic carbon nitride by a simple method and cheap reactant; (ii) Characterization of P-doped g-C_3N_4 by FTIR, SEM, XRD, EDX and BET analyses; (iii) The effect of factors such as pH, doses of adsorbent, methylene blue (MB), time and temperature; (iv) Studying kinetic and isotherm models.

MATERIALS AND METHODS

Chemicals

Melamine, sodium hydroxide, methylene blue, hydrochloric acid (37%) and phosphoric acid (85%) were purchased from Merck and Loba Chemie Pvt. Ltd. (India). These chemicals were used without any further purification.

Characterization

Melting points were measured on an Electrothermal 9100 apparatus. FT-IR spectra were recorded on Unicam Galaxy 5000. Scanning electron microscopy (SEM) study in the present work was performed by FE-SEM (Tescan-Chek). Wide-angle X-ray diffraction (XRD) measurements were performed at room temperature on XPertPro using Cu-Kα radiation (λ = 1.54 Å). UV-Vis spectroscopy was conducted by a Hitachi UV-365 spectrophotometer. The nitrogen adsorption-desorption isotherms were measured by Belsorp Mini II and Bel Prep VAC II. The concentration of MB was obtained by a UV-Vis spectrophotometer (λ_{max} = 665 nm).

Preparation of P-doped Graphitic Carbon Nitride

The P-doped graphitic carbon nitride was synthesized by a simple process. First, 5 g of melamine was mixed with 100 ml aqueous solution of phosphoric acid (2% v/v) and was stirred at 25 °C for 1 h. After water evaporation at 100 °C for 2 h, to complete the reaction, the mixture was heated up to 550 °C for 1 h. Finally, the P-doped graphitic carbon nitride product was collected and ground into powder. The synthesized composite was characterized using the techniques cited above.

Adsorption Experiments

To evaluate the performance of P-doped graphitic carbon nitride, the methylene blue was chose as an organic pollutant. The adsorption activity of the P-doped graphitic carbon nitride (0.01-0.25 g) was studied by adsorption of methylene blue (2-22 ppm) under different conditions such as pH (2-12), time (30-300 min) and temperatures (15-45 °C). At a certain time, 10 ml suspension mixture of the composite and MB were sampled and centrifuged (VS4000C, 4000 rpm) to remove the particles. The concentration of the MB was analyzed by the UV-Vis spectrophotometer (λ_{max} = 665 nm).

The amount of MB adsorbed was calculated by Eqs. ((1) and (2));

$$q_e = \frac{(C_i - C_e)V}{m} \quad (1)$$

$$R_e = \frac{(C_i - C_f)V}{C_i} \times 100 \quad (2)$$

where q_e (mg g^{-1}) is the amount of the MB adsorbed per unit mass of g-C_3N_4. C_i, C_e and C_f represent the initial, equilibrium and final concentration (mg l^{-1}), respectively, v denotes the volume (l) of the solution, and m is the mass (g) of P-g-C_3N_4.

The optimum pH test (1): The pH of solution was

Table 1. The Conditions of MB Adsorption on P-g-C_3N_4

Test	pH	Dosage of adsorbent (g)	Initial MB concentration (ppm)	Time (min)	Temperature (°C)
1	2-12	0.09	10	90	23
2	8	0.01-0.25	10	90	23
3	8	0.07	2-22	90	23
4	8	0.07	8	60	23
5	8	0.07	8	60	23
6	8	0.07	8	60	18

adjusted ranged from 2.0-12.0 using 0.1 M of NaOH or HCl solutions. The experiment was carried out to find out the optimum pH. The conditions of tests are shown in Table 1.

The optimum dosage of adsorbent test (2): The experiments were carried out to find out the optimal dosage of adsorbent for the removal of methylene blue from the aqueous solutions in the range of (0.01-0.25 g).

The initial MB concentration test (3): The effect of initial MB concentration in the range of 2-22 ppm on adsorption was investigated under the specified conditions.

The optimum time test (4): To find out the equilibrium time for the removal of MB, the range of 30-360 min was studied.

The temperature effect test (5): The effect of temperature in the range of 15-45 °C on adsorption was investigated under the determined conditions (Table 1).

The reusability test (6): After adsorption of MB from aqueous solution, the P-doped graphitic carbon nitride can be recovered in concentrated ethanol solution. After desorption of MB, P-g-C_3N_4 is able to absorb MB.

The adsorption kinetic data of methylene blue (MB) was analyzed using two kinetics models including pseudo-first order and pseudo-second order rate equations [19,20]. The pseudo-first order kinetics rate Eq. (3) is expressed as follows:

$$\ln(q_e - q_t) = \ln q_e - k_1 t \quad (3)$$

q_e and q_t (mg g^{-1}) represent the amount of MB, and K_1 shows the rate constant (1 min^{-1}) (slope of the linear plot of $\log(q_e - q_t)$ *vs.* t). The pseudo-second-order reaction rate equation was employed to assess the kinetics of methylene blue adsorption on P-g-C_3N_4. Eq. (4) is as follows:

$$\frac{t}{q_t} = \frac{1}{k_2 q_e^2} + \frac{t}{q_e} \quad (4)$$

q_e and q_t (mg g^{-1}): the amount of methylene blue adsorbed by P-g-C_3N_4 nanosheet

K_2: the rate constant of pseudo-second- order adsorption (g mg^{-1} min^{-1}).

Kinetics measurements were performed in a glass vessel equipped with a mechanical stirrer in static conditions. The optimum dose of 0.07 of adsorbent was contacted with concentration 2-8 ppm of MB. The concentration of MB from the aqueous solution was determined at known time intervals. The analysis of MB was performed by a UV-Vis spectrophotometer (λ_{max} = 665 nm).

One of the important factors in the design of adsorption systems is the adsorption isotherm. The isotherms can provide useful information about adsorption capacity of adsorbent, multilayer or monolayer formation, and type of interaction. In this study, the Langmuir and Freundlich adsorption isotherms were selected based on the literature [21-25]. These isotherms are the most employed models for description the equilibrium distribution of methylene blue on surfaces. The heterogeneity of the adsorbent surface can be calculated by the Freundlich adsorption isotherm model

based on the multilayer adsorption. The Freundlich Eq. (5) can be written as [26]:

$$\ln q_e = \ln K_f + \frac{1}{n} \ln C_e \quad (5)$$

K_f and n are constants for a given adsorbate and adsorbent. The graph was plotted and the slop and intercept were obtained to determine the value of K_f and n by the plot including $\ln q_e$ *vs*. $\ln C_e$. The amount of $n > 1$ suggests favorable adsorption conditions. The Langmuir adsorption isotherm model is used to describe that only one molecule can bind to each site of the adsorbent. Homogeneous sites and monolayer adsorption occur in the Langmuir adsorption. The Langmuir's Eq. (6) can be written as [27]:

$$\frac{C_e}{q_e} = \frac{1}{q_{\max} b} + \frac{C_e}{q_{\max}} \quad (6)$$

q_e: the adsorbent amount (mg g^{-1}) of the methylene blue; C_e: the equilibrium concentration of the methylene blue in the solution (mg l^{-1}); q_m: monolayer adsorption capacity (mg g^{-1}); b: the constant related to the free energy of adsorption (l mg^{-1}).

RESULTS AND DISCUSSION

Characterization of the P-doped Graphitic Carbon Nitride

Figure 1 displays the FT-IR spectrum of P-g-C_3N_4. The aromatic C-N heterocycles are observed within 1200-1687 cm^{-1} and at 3152 cm^{-1} [28]. The stretching pick at 808 cm^{-1} is assigned to the C-N plane bending [29]. The spectrum of prepared P-g-C_3N_4 has partial different rather to graphitic carbon nitride, given the absence of major changes to the framework and existence of a little amount of phosphorus atom.

Figure 2 demonstrates the XRD patterns of g-C_3N_4 and P-g-C_3N_4. The peaks at 13.5° and 27.4° in non-doped g-C_3N_4 and doped g-C_3N_4 can be attributed to (100) and (002) reflections (JCPDS 87-1526: Reference card of g-C_3N_4). The (100) plane is shown an in-plane structural packing motif. The weaker peak for the P-g-C_3N_4 is determined the decrease planar size of the layers. It revealed the same peaks at both of them and it was observed that the phosphorus doping cannot disrupt the pure product [14]. The size of composite was obtained as 8.3 nm.

In Fig. 3, the SEM images of g-C_3N_4 and P-g-C_3N_4 are exhibited. The surface of g-C_3N_4 can be seen in Fig. 3a. The different crystals stacking layers with smooth surface can be seen in Fig. 3b. In images of P-g-C_3N_4, the layers have become thinner and curlier (Fig. 3c). After addition of phosphorus, some nanoparticles agglomeration was observed on the surface of g-C_3N_4 (Fig. 3d). These images confirm the p-doping on the surface of graphitic carbon nitride by thinner and curlier layers rather to g-C_3N_4.

The energy dispersive X-ray analyzer spectroscopy (EDX or EDA) can provide useful information about elemental analysis. It is an essential part of a SEM [30]. The analysis was performed to further validation of the combination of g-C_3N_4 and phosphorus, Figs. 4-5. The SEM image of P-g-C_3N_4 is seen in Fig. 4a. The corresponding EDS mappings to this image are shown in Figs. 4b-5.

The mappings of C and N elements are seen in Fig. 4b and Fig. 5a, confirming the g-C_3N_4 structure. The maps in Fig. 5b illustrate that P atoms are in a close contact with g-C_3N_4. It is also observed the uniform distribution of P elements in g-C_3N_4. Figures 4b-5 can demonstrate that C, N and P are distributed homogeneously within graphitic carbon nitride.

The physical adsorption can be explained by Brunauer-Emmett-Teller (BET) theory to achieve the type of pores, hysteresis, pore size distribution and the specific surface area of materials. The BET surface area measurement was performed using an adsorption-desorption isotherm (nitrogen). The nitrogen adsorption-desorption isotherm is shown for P-g-C_3N_4 in Fig. 6. The specific surface areas, cumulative pore volume and pore sizes were obtained as 33.123 $m^2 g^{-1}$, 0.2996 $cm^3 g^{-1}$ and 36.176 nm. The specific surface areas of P-g-C_3N_4 was increased compared to g-C_3N_4 (25.1 $m^2 g^{-1}$). The IV type isotherm was investigated according to the IUPAC classification which confirmed a porous surface [31-33].

The IV type isotherm demonstrates porous adsorbents with pores in the range of 1.5-100 nm and capillary condensation is accompanied by hysteresis. It occurs near completion of the first monolayer. Hysteresis loop is the H1

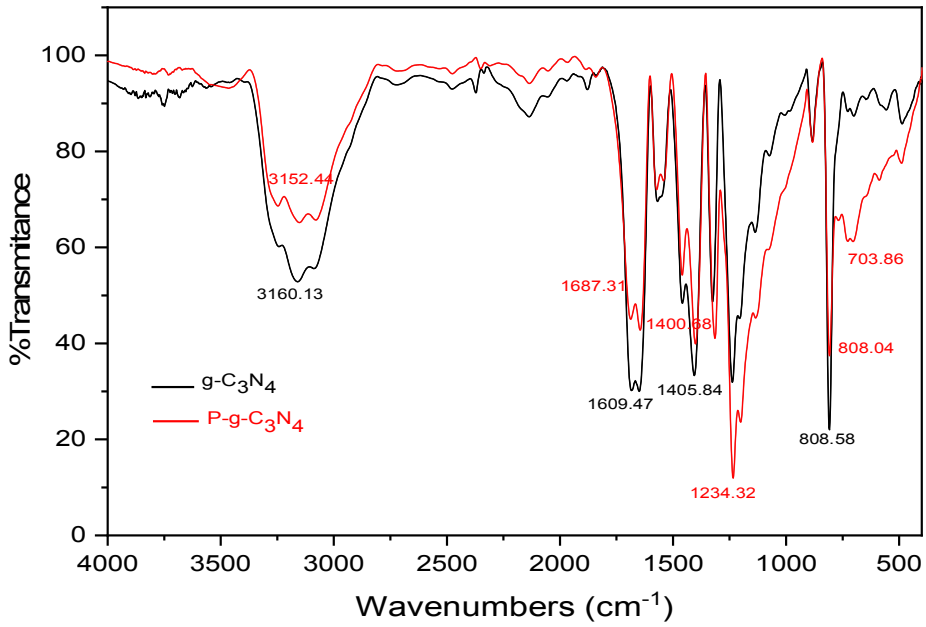

Fig. 1. The FT-IR spectra of g-C_3N_4 and P-g-C_3N_4.

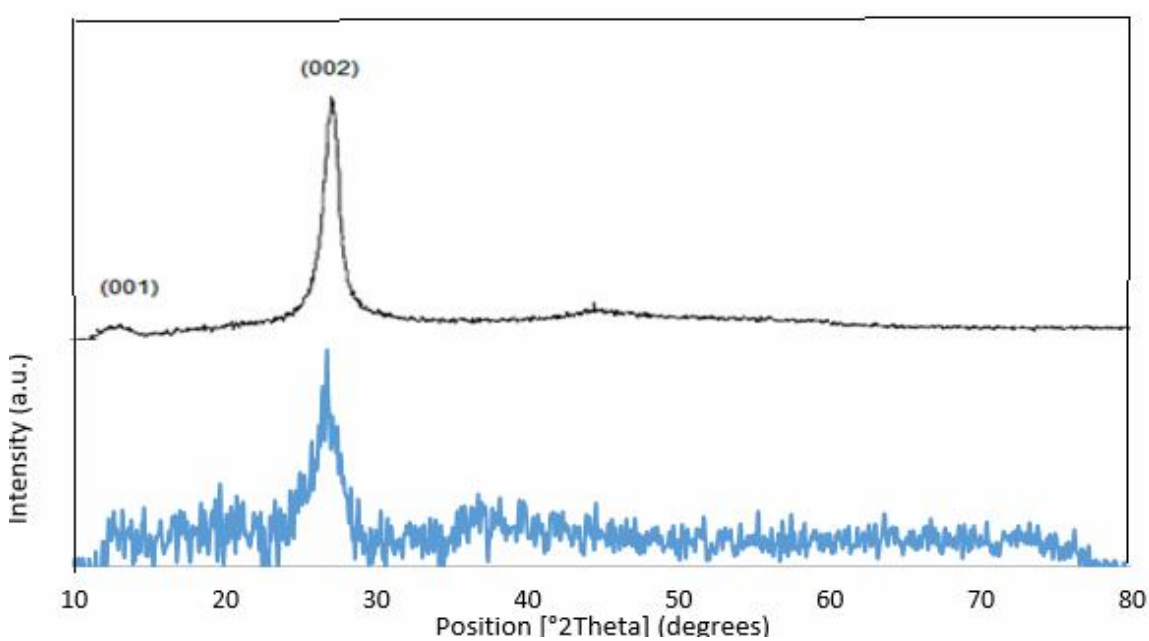

Fig. 2. The XRD patterns of a) g-C_3N_4 and b) P-g-C_3N_4.

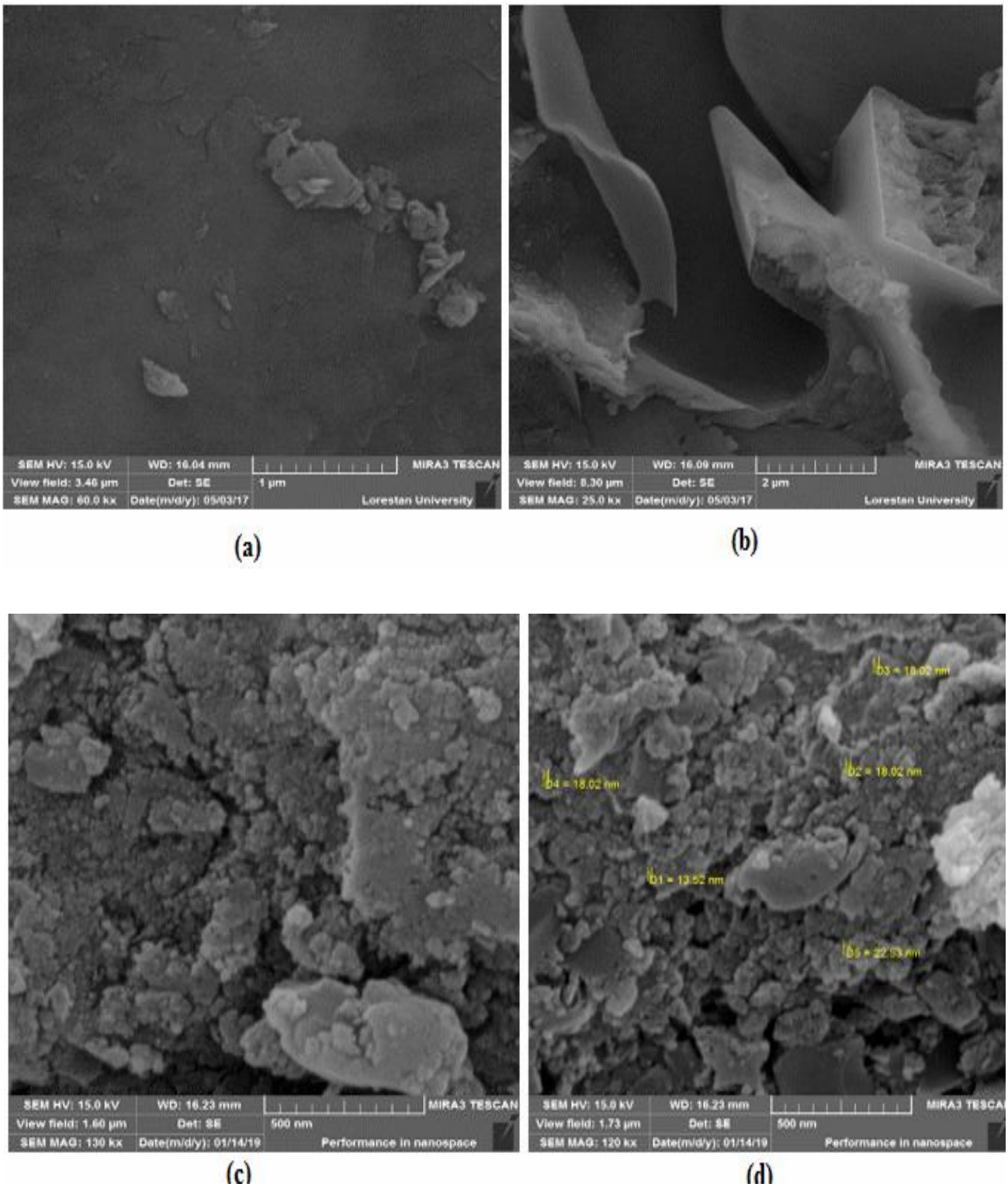

Fig. 3. The SEM images of (a,b) g-C_3N_4 and (c,d) P-g-C_3N_4.

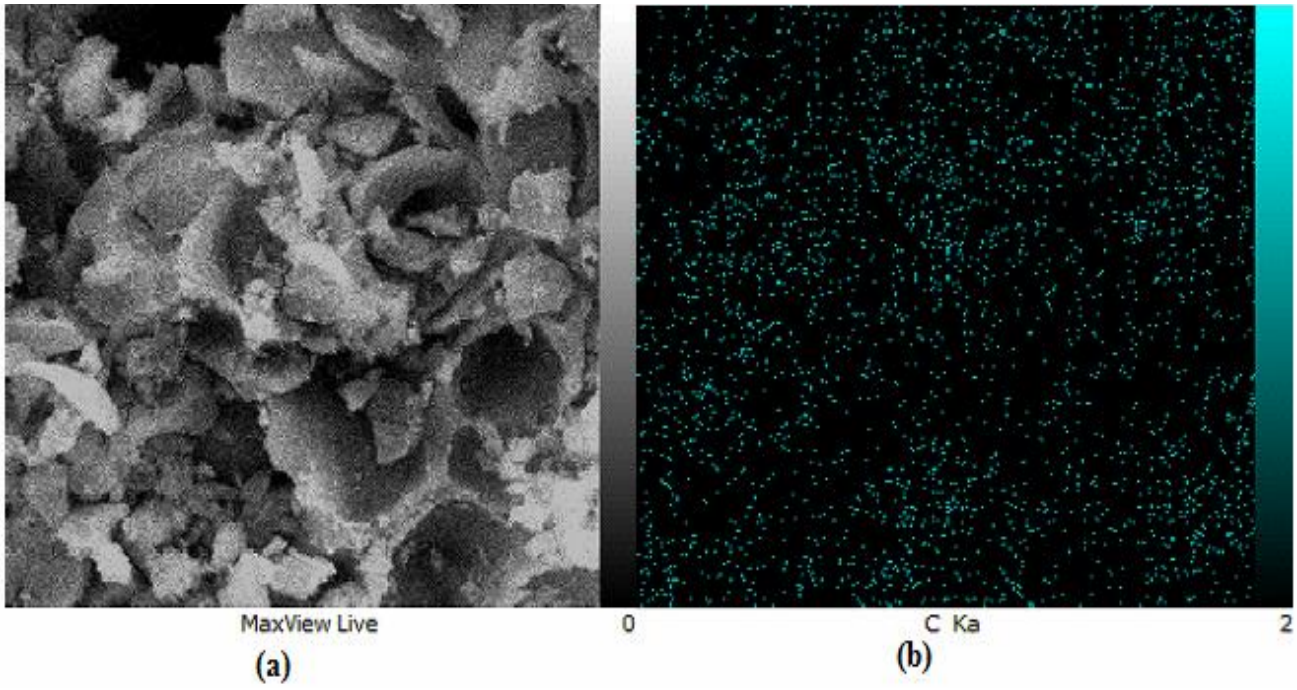

Fig. 4. (a) The SEM of P-g-C_3N_4 and (b) the EDS elemental distributions of C in P-g-C_3N_4.

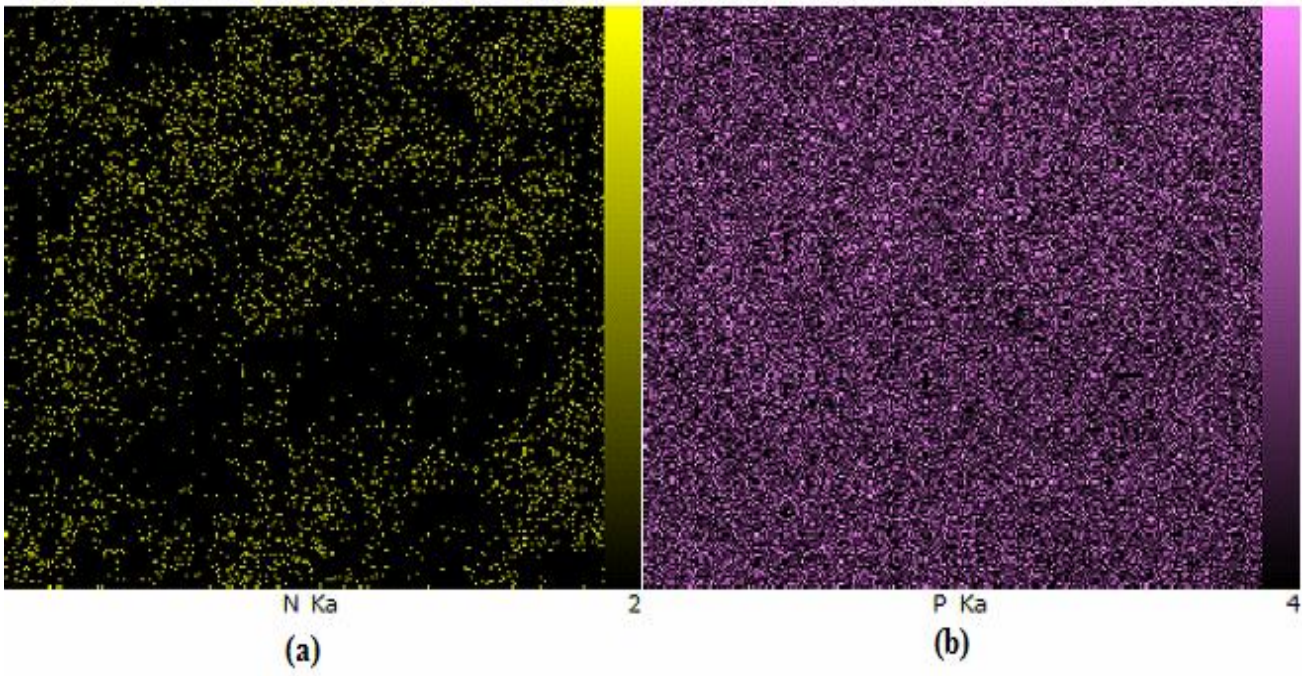

Fig. 5. The EDS elemental distributions of (a) N atoms and (b) P atoms in P-g-C_3N_4.

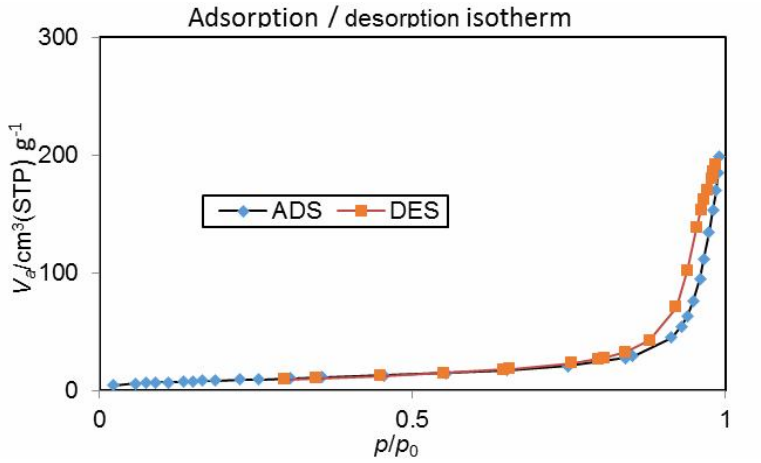

Fig. 6. The N_2 adsorption-desorption isotherm.

type that indicates a narrow range of uniform mesopore [34].

ADSORPTION STUDIES

Effects of Different Parameters on the Adsorption

The pH effect. The pH has an important role on the adsorption of material because the adsorbent surface can be either protonated or deprotonated by hydrogen or hydroxide. The condition on adsorbent surface can cause adsorption or desorption, affecting on removal of MB [15]. The pH effect on the adsorption of MB is shown in Fig. 7. The optimum pH was obtained at 8. It can be seen that as the pH values increased, so did the efficiency of removal. Therefore, the best results were obtained at alkaline pH. Indeed, the increase in % adsorption is due to the deportation of g-C_3N_4 in basic condition. Therefore, the positively charged dyes such as methylene blue can be adsorbed at alkaline pH.

The effect of adsorbent doses. The role of the adsorbent amount can be seen in Fig. 7b that the maximum efficiency was obtained at 0.07 g of P-g-C_3N_4. The adsorption percentage remained constant by increasing the adsorbent mass because of the saturation of P-g-C_3N_4 surface.

The methylene blue concentration. The study of the MB dose effect on the adsorption is particularly important because it can explain the adsorbent-adsorbate interaction in solution. The high concentration of MB can produce pollution. The optimum concentration of MB is an important parameter for adsorption on P-g-C_3N_4. In Fig. 8a, the optimum dose of methylene blue was found as 8 ppm. By increasing the amount of MB, the recovery percentage was increased until the activity sites were saturated, since then, the addition of MB concentration did not have a positive effect on recovery percentage of MB at a constant dosage of adsorbent.

The contact time. In the batch experiment, time has an important role in the adsorption. The completion of adsorption time affects the efficiency adsorption. When the contact time between MB and adsorbent was low, the adsorption was decreased and the dye could remain in solution. According to the experiments, the optimum time for equilibrium was achieved at 60 min. Initially, the efficiency removal was enhanced sharply until the surface of P-g-C_3N_4 was saturated. Because the first time, there are not equilibrium between constant dosage of MB and P-g-C_3N_4 in solution. After 60 min, the removal of dye could not improve significantly due to the saturation of the adsorbent surface (Fig. 8b).

The temperature. The adsorption process can also be affected by the temperature. Nevertheless, according to Fig. 9, increasing the temperature leads to a decrease in adsorption percentage since this adsorption process is exothermic. Based on the results, the nature of MB adsorption on P-g-C_3N_4 is physisorption [35], therefore the elevation of optimum temperature can consume energy.

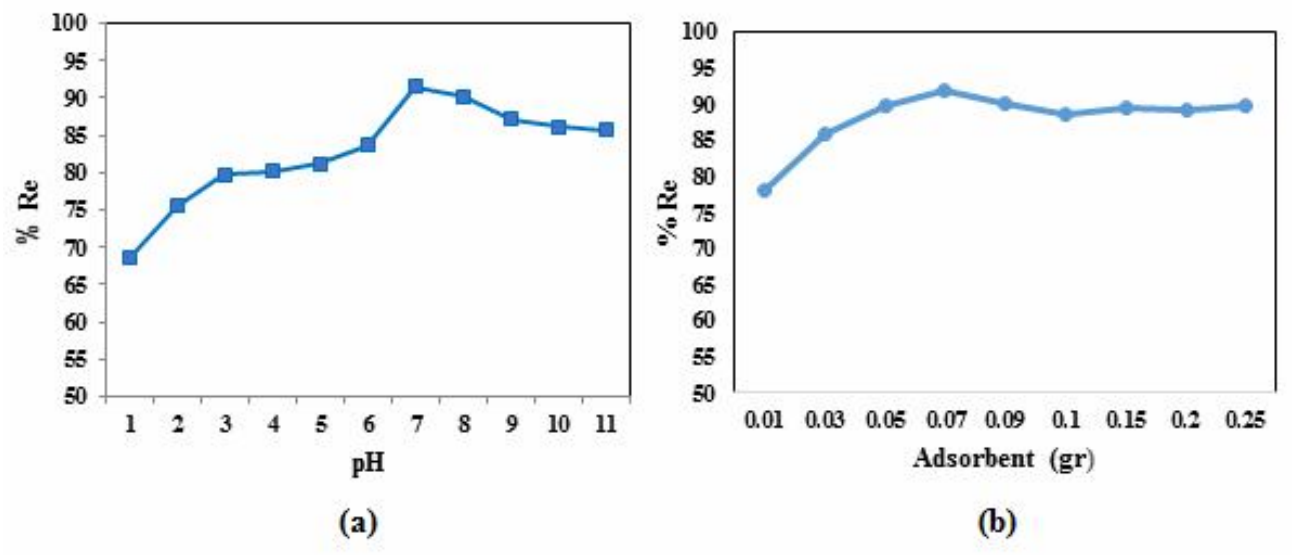

Fig. 7. The effect of a) pH and b) adsorbent doses of methylene blue (MB) on P-g-C_3N_4.

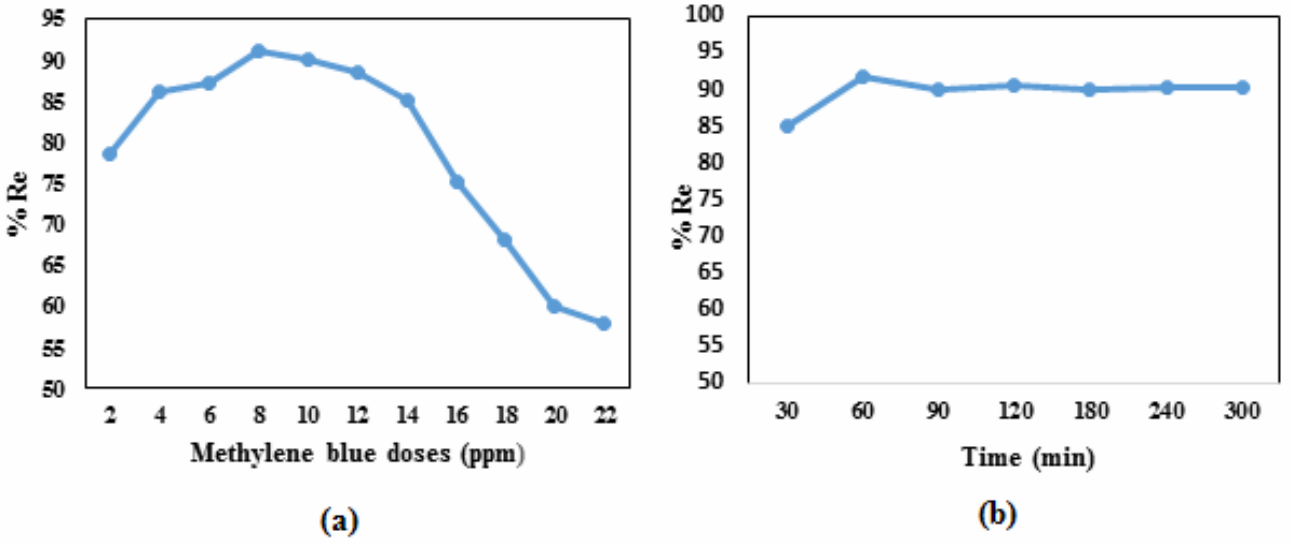

Fig. 8. The effect of a) concentration of MB and b) time of the MB adsorption on P-g-C_3N_4.

Adsorption Kinetics Studies

The kinetics plots were plotted for different initial concentrations (Fig. 10). Slope and intercept values corresponded to pseudo-second-order equation.

Adsorption Isotherm Studies

The plot of Q_e *vs.* C_e is shown in Fig. 11a. The Freundlich and Langmuir isotherms are shown in Figs. 11b-c. The values of the Freundlich and Langmuir constant are reported in Table 2. The Freundlich isotherm model shows a regression coefficient R^2 = 0.97 (Fig. 11b). The Langmuir's graph was plotted by Ce/q_e *vs*. *Ce* (Fig. 11c). The regression coefficient (R^2) for Langmuir isotherm was obtained 0.98. According to the Langmuir's equation, the slop and

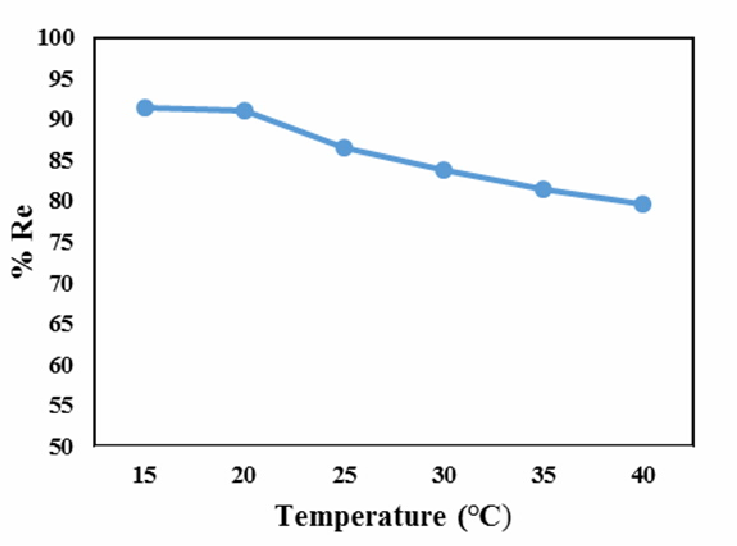

Fig. 9. The effect of temperature on the methylene blue (MB) adsorption on P-g-C_3N_4.

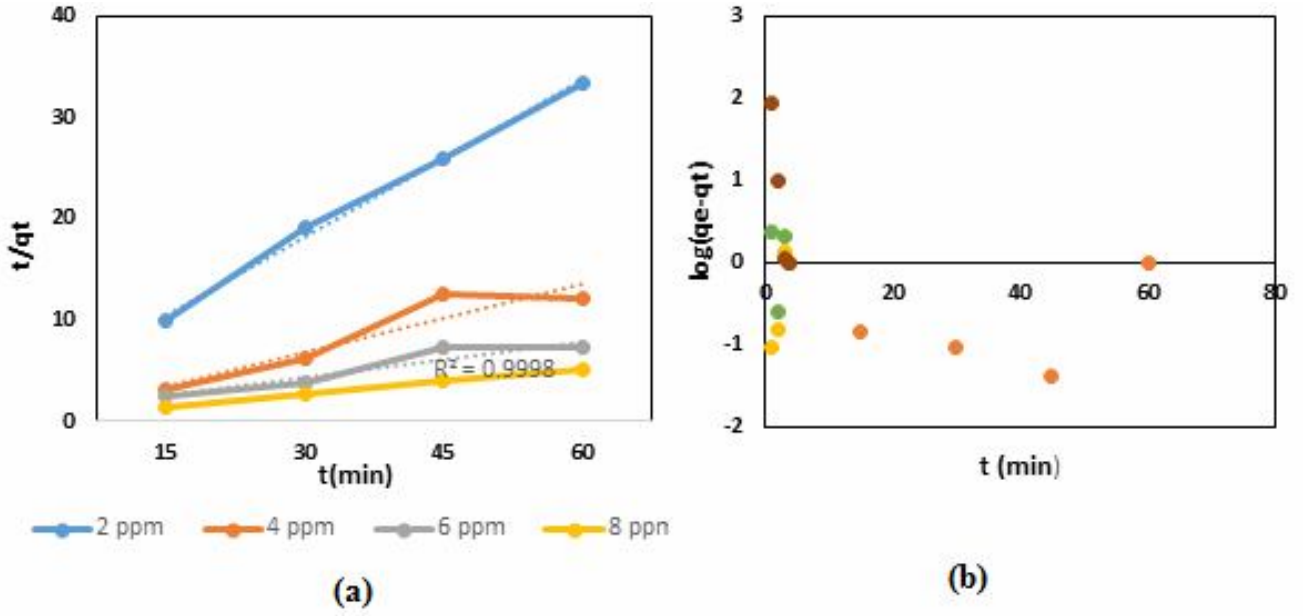

Fig. 10. Pseudo-second-order kinetics (a) and pseudo-first-order kinetics (b) of MB adsorption on P-g-C_3N_4 nanosheet.

intercept of the graph indicate the values of q_{max} and K_l.

The process of methylene blue adsorption followed the Langmuir's model (R^2 = 0.98) and the higher adsorption capacity. Homogeneous sites and monolayer adsorption occur in the Langmuir adsorption.

Recyclability

The recyclability of P-g-C_3N_4 is an important factor due to its low cost and high efficiency. The results indicate the reusability of composite after five times, suggesting that it can be an environmentally friendly material for the purification of wastewater (Fig. 12).

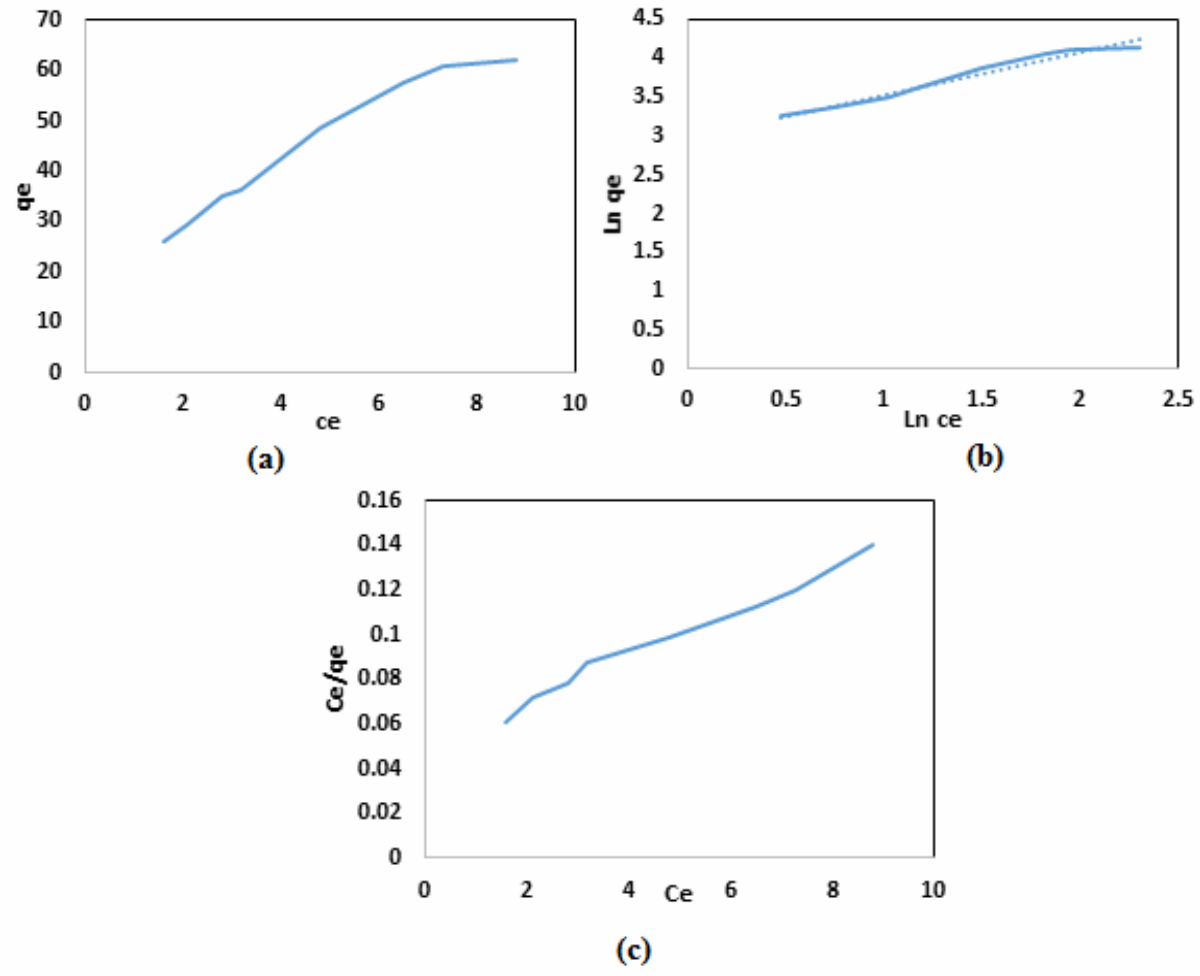

Fig. 11. a) The fitting results (q_e/c_e); b) Freundlich and c) Langmuir models for MB adsorption on P-g-C_3N_4.

Table 2. Information of Isotherm Models for MB Adsorption on P-g-C_3N_4

Freundlich			Langmuir		
K_f (mg l^{-1})	n	R^2	Q_{max} (mg g^{-1})	K_l (l mg^{-1})	R^2
19.88	1.84	0.97	100	0.005	0.98

CONCLUSIONS

In this research, we used a gentle strategy for preparation of P-doped graphitic carbon nitride as an adsorbent. The melamine and phosphoric acid were applied for this efficient synthesis method. The structure of P-g-C_3N_4 was confirmed by analysis methods including FT-IR, XRD, SEM and BET. The efficiency of P-g-C_3N_4 for adsorption of

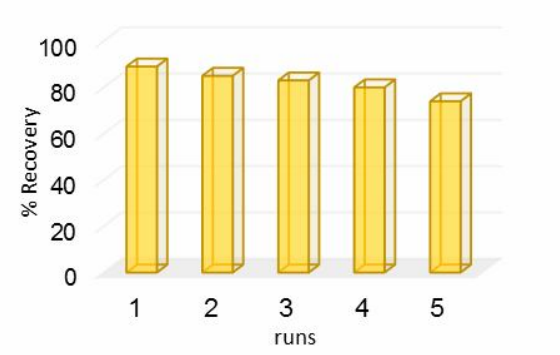

Fig. 12. The reusability of MB.

methylene blue was further studied. The operational conditions including pH, methylene blue concentration, adsorbent doses, time and temperature were tested. The results offered the optimum conditions to achieve the best yield. The suitable kinetics was found to be pseudo-second-order kinetic. The Langmuir model corresponded to the equilibrium experiments. The utilized P-g-C_3N_4 could be recovered and retained after five times use. These findings suggest the suitability of our novel strategy for synthesis of P-g-C_3N_4 for adsorption of organic pollutants.

REFERENCES

[1] Low, J.; Cao, S.; Yu, J.; Wageh, S., Two-dimensional layered composite photocatalysts. *Chem. Commun.* **2014**, *50*, 10768-10777, DOI: 10.1039/c4cc02553a.

[2] Butchosa, C.; McDonald, T. O.; Cooper, A. I.; Adams, D. J; Zwijnenburg, M. A., Shining a light on s-Triazine-based polymers. *J. Phys. Chem. C.,* **2014**, *118*, 4314-4324, DOI: 10.1021/jp411854f.

[3] Liebig, J. V., About some nitrogen compounds. *Ann. Pharm.* **1834**, *10*, 1-47, DOI: 10.1002/ jlac.18340100102.

[4] Hong, J.; Yin, S.; Pan, Y.; Han, J.; Zhou, T.; Xu, R., Porous carbon nitride nanosheets for enhanced photocatalytic activities. *Nanoscale,* **2014**, *6*, 2315-23216, DOI: 10.1039/c4nr05341a.

[5] Hong, J.; Xia, X.; Wang, Y.; Xu, R., Mesoporous carbon nitride with *in situ* sulfur doping for enhanced photocatalytic hydrogen evolution from water under visible light. *J. Mater. Chem.* **2012**, *22*, 15006-15012, DOI: 10.1039/c2jm32053c.

[6] Zhu, J.; Xiao, P.; Li, H.; Carabineiro, S. A. C., Graphitic carbon nitride: synthesis, properties, and applications in catalysis. *ACS Appl. Mater. Inter.* **2014**, *6*, 16449-16465, DOI: 10.1021/am502925j.

[7] Maeda, K.; Sekizawa, K.; Ishitani, O., A polymeric-semiconductor-metal-complex hybrid photocatalyst for visible-light CO_2 reduction. *Chem. Commun.* **2013**, *49*, 10127-10129, DOI: 10.1039/c3cc45532g.

[8] Wang, S.; Lin, J.; Wang, X., Semiconductor-redox catalysis promoted by metal-organic frameworks for CO_2 reduction. *Phys. Chem. Chem. Phys.* **2014**, *16*, 14656-14660, DOI: 10.1039/c4cp02173h.

[9] Hong, Y.; Jiang, Y.; Li, C.; Fan, W.; Yan, X.; Yan, M.; Shi, W., In-situ synthesis of direct solid-state Z-scheme V_2O_5/g-C_3N_4 heterojunctions with enhanced visible light efficiency in photocatalytic degradation of pollutants. *Appl. Catal. B-Environ.* **2016**, *180*, 663-673, DOI: 10.1016/j.apcatb.2015.06.057.

[10] Kong, H. J.; Won, D. H.; Kim, J.; Woo, S. I., Sulfur-doped g-C_3N_4/$BiVO_4$ composite photocatalyst for water oxidation under visible light. *Chem. Mater.* **2016**, *28*, 1318-1324, DOI: 10.1021/ acs.chemmater.5b04178.

[11] Wang, Y.; Wang, Z.; Muhammad, S.; He, J., Graphite-like C_3N_4 hybridized $ZnWO_4$ nanorods: Synthesis and its enhanced photocatalysis in visible light. *Cryst. Eng. Comm.* **2012**, *14*, 5065-5070., DOI: 10.1039/c2ce25517k.

[12] Pan, C.; Xu, J.; Wang, Y.; Li, D.; Zhu, Y., Dramatic activity of C_3N_4/$BiPO_4$ photocatalyst with core /shell structure formed by self-Assembly. *Adv. Funct. Mater.* **2012**, *22*, 1518-1524, DOI: 10.1002/

adfm.201102306.

[13] Shcherban, N. D.; Filonenko, S. M.; Ovcharov, M. L.; Mishura, A. M.; Skoryk, M. A.; Aho, A.; Murzin, D. Y., Simple method for preparing of sulfur-doped graphitic carbon nitride with superior activity in CO_2 photoreduction. *Chem. Select*, **2016**, *1*, 4987-4993, DOI: 10.1002/slct.201601283.

[14] Liu, S.; Zhu, H.; Yao, W.; Chen, K.; Chen, D., One step synthesis of P-doped g-C_3N_4 with the enhanced visible light photocatalytic activity. *Appl. Surf. Sci.,* **2018**, *430*, 309-315, DOI: 10.1016/j.apsusc.2017.07.108.

[15] Fronczak, M.; Krajewska, M.; Demby, K.; Bystrzejewski, M., Extraordinary adsorption of methyl blue onto sodium-doped graphitic carbon nitride. *J. Phys. Chem. C,* **2017**, *121*, 15756-15766, DOI: 10.1021/acs.jpcc.7b03674.

[16] Ge, L.; Han, C.; Xiao, X.; Guo, L.; Li, Y., Enhanced visible light photocatalytic hydrogen evolution of sulfur-doped polymeric g-C_3N_4 photocatalysts. *Mater. Res. Bull.,* **2013**, *48*, 3919-3925, DOI: 10.1016/j.materresbull.2013.06.002.

[17] Dong, G.; Zhang, L., Porous structure dependent photoreactivity of graphitic carbon nitride under visible light. *J. Mater. Chem.,* **2012**, *22*, 1160-1166, DOI: 10.1039/c1jm14312c.

[18] Zhang, Y.; Mori, T.; Ye, J.; Antonietti, M., Phosphorus-doped carbon nitride solid: Enhanced electrical conductivity and photocurrent generation. *J. Am. Chem. Soc.,* **2010**, *132*, 6294-6295, DOI: 10.1021/ja101749y.

[19] Lagergren, S. K., About the theory of so-called adsorption of soluble substances, *Kungliga Svenska Vetenskapsakademens Handlingar* **1898**, *24*, 1-39.

[20] Ho, Y. S.; McKay, G., The kinetics of sorption of divalent metal ions onto sphagnum moss peat, *Water Res.,* **2000**, *34*, 735-742, DOI: 10.1016/S0043-1354(99)00232-8.

[21] Rezakazemi, M.; Shirazian, S., Lignin-chitosan blend for methylene blue removal: Adsorption modeling, *J. Mol. Liq.,* **2019**, *274*, 778-791, DOI: 10.1016/j.molliq.2018.11.043.

[22] Hajam, M.; Idrissi Kandri, N.; Harrach, A.; El khomsi, A.; Zerouale, A., Adsorption of methylene blue on industrial softwood waste "Cedar" and hardwood waste "Mahogany": comparative study. *Materials Today: Proceedings* **2019**, *13*, 812-821. DOI: 10.1016/j.matpr.2019.04.044.

[23] Wang, Z.; Gao, M.; Li, X.; Ning, J.; Zhou, Z.; Li, G., Efficient adsorption of methylene blue from aqueous solution by graphene oxide modified persimmon tannins, *Mater. Sci. Eng. C.,* **2019**, 110196. DOI: 10.1016/j.msec.2019.110196.

[24] Bergaoui, M.; Nakhli, A.; Benguerba, Y.; Khalfaoui, M.; Erto, A.; Soetaredjo, F. E.; Ismadji, S.; Ernst, B., Novel insights into the adsorption mechanism of methylene blue onto organo-bentonite: Adsorption isotherms modeling and molecular simulation, *J. Mol. Liq.,* **2018**, *272*, 697-707, DOI: 10.1016/j.molliq.2018.10.001.

[25] Jaseela, P. K.; Garvasis, J.; Joseph, A., Selective adsorption of methylene blue (MB) dye from aqueous mixture of MB and methyl orange (MO) using mesoporous titania (TiO_2)-poly vinyl alcohol (PVA) nanocomposite. *J. Mol. Liq.,* **2019**, *286*, 110908, DOI: 10.1016/j.molliq.2019.110908.

[26] Van der Bruggen, B., Freundlich Isotherm. In Encyclopedia of Membranes, Drioli, E.; Giorno, L., Eds. Springer Berlin Heidelberg: Berlin, Heidelberg, 2015, p. 25-60.

[27] Langmuir, I., The adsorption of gases on plane surfaces of glass, mica and platinum. *J. Am. Chem. Soc.,* **1918**, *40*, 1361-1403. DOI: 10.1021/ja02242a004.

[28] Li, Y.; Zhang, J.; Wang, Q.; Jin, Y.; Huang, D.; Cui, Q.; Zou, G., Nitrogen-rich carbon nitride hollow vessels: synthesis, characterization, and their properties. *J. Phys. Chem. B,* **2010**, *114*, 9429-9434, DOI: 10.1021/jp103729c.

[29] Lotsch, B. V.; Döblinger, M.; Sehnert, J.; Seyfarth, L.; Senker, J.; Oeckler, O.; Schnick, W., Unmasking melon by a complementary approach employing electron diffraction, solid-state NMR spectroscopy, and theoretical calculations-structural characterization of a carbon nitride polymer. *Chem. Eur. J.,* **2007**, *13*, 4969-4980, DOI: 10.1002/chem.200601759.

[30] Goldstein, J., Scanning electron microscopy and X-Ray microanalysis. Springer, 2003, p. 21-60.

[31] Brunauer, S.; Emmett, P. H.; Teller, E., Adsorption of gases in multimolecular layers. *J. Am. Chem. Soc.,* **1938**, *60*, 309-319, DOI:10.1021/ja01269a023.

[32] Sing, K. S.; Everett, W. D. H.; Haul, R. A. W.; Moscou, L.; Pierotti, R. A.; Rouquerol J.; Siemieniewska, T., Reporting physisorption data for gas/solid systems with special reference to the determination of surface area and porosity, *Pure Appl. Chem. Vol.* **1985**, *57*, 603-619, DOI: 10.1351/pac198557040603.

[33] Talip, Z.; Eral, M.; Hiçsönmez, U., Adsorption of thorium from aqueous solutions by perlite. *J. Environ. Radioact.* **2009**, *100*, 139-143, DOI: 10.1016/j.jenvrad.2008.09.004.

[34] Lowell, S.; Shields, J.; Thomas, M. A.; Thommes, M., Characterization of Porous Solids and Powders: Surface Area. Porosity and Density, Springer, 2004, p. 11-14.

[35] Torres-Knoop, A.; Poursaeidesfahani, A.; Vlugt, T. J. H.; Dubbeldam, D., Behavior of the enthalpy of adsorption in nanoporous materials close to saturation conditions, *J. Chem. Theory. Comput.,* **2017**, *13*, 3326-3339, DOI: 10.1021/acs.jctc.6b01193.